Type of contribution:
Editorial
▶ Research Paper
Case Study
Review Paper
Scientific Data
Report of Tech. Application

e-issn. 2798-5245

Mechanical Engineering for Society and Industry
Vol. 5, No. 1 (2025) pp 257-267
https://doi.org/10.31603/mesi.13234

Exploring the potential of indonesian iron sand in the formation of iron nitride for magnetic applications

Indra Sidharta[1], Rakhasoni Firman Syah[2], Sutikno[1], Darminto[2], Abdullah Shahab[1]*

[1] Department of Mechanical Engineering, Institut Teknologi Sepuluh Nopember, Surabaya 60111, **Indonesia**
[2] Department of Physics, Institut Teknologi Sepuluh Nopember, Surabaya 60111, **Indonesia**
✉ shahab_nqa@yahoo.com

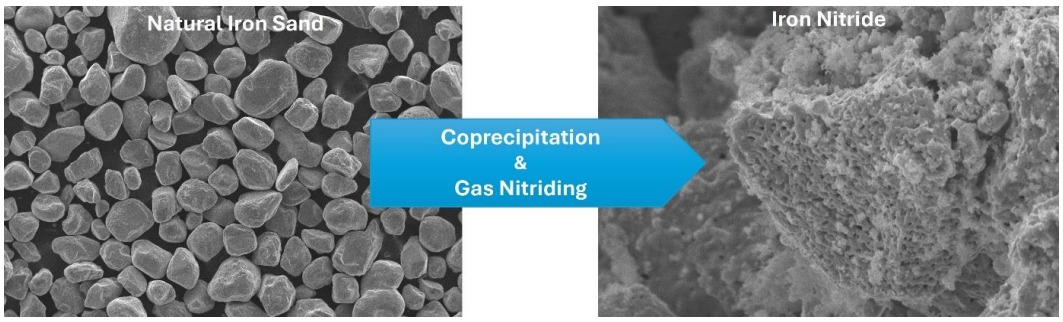

Highlights:

- Iron nitride materials were developed from Indonesian natural iron sands using subsequent coprecipitation and gas nitriding processes.
- Fe_3O_4 and Fe_2O_3 nanopowder synthesized from natural iron sands can be used as a precursor material for iron nitride.
- Gas nitriding of Fe_3O_4 powder results in the formation of both the Fe_4N and Fe_3N phases, achieving a maximum magnetic saturation of 75.41 emu/g.

Abstract

Iron nitride is a transition metal material that exhibits ferromagnetic properties at room temperature, making it a suitable candidate for use in Soft Magnetic Composites (SMC) applications. Previous research showed that iron nitride can be synthesized using nano-sized iron oxide powder derived from processed natural iron sand through gas nitriding. Considering the abundance of iron sand in Indonesia, there is a need to carry out an investigation related to iron sand-based SMC. Therefore, this research aims to synthesize iron nitride material using the abundant natural iron sand discovered in Indonesia. This study used iron oxide material synthesized from locally obtained natural iron sand, in the form of Fe_3O_4 and Fe_2O_3. Iron oxide undergoes coprecipitation and was subsequently exposed to the gas nitriding process with a holding time of 4 hours and a gas flow of 150 mL/min in NH_3 gas. The results show that iron nitride is formed after nitriding of iron oxide powders, and the phases formed include ε-Fe_3N and γ'-Fe_4N. The synthesized material exhibits soft magnetic properties, with saturation magnetization values ranging from the highest at 75.41 emu/g and the lowest at 18.9 emu/g.

Keywords: Natural iron sand; Iron nitride; Iron oxide; Nitriding; Soft magnet

Article info
Submitted: 2025-02-27
Revised: 2025-06-06
Accepted: 2025-06-22

Publisher
Universitas Muhammadiyah Magelang

1. Introduction

Indonesia's transition to electric vehicles (EVs) is fostering a thriving ecosystem that offers promising opportunities for all stakeholders. The development of the EVs industry has driven extensive research aimed at achieving technological breakthroughs and ensuring self-reliance in innovation [1], [2], [3]. One key area of research is electric motors, specifically axial flux motors. This type of motor holds promising technological and business impact on EVs. The impact of axial flux motor technology on the EVs industry is exemplified by the acquisition of YASA, a spin-off company from Oxford University, by the Mercedes-Benz Group in 2021 [4], [5].

Research on axial flux motors has also been carried out in Indonesia [6], [7], [8]. However, most of the components were imported from the international market. One of the key components that determine the performance of an axial flux motor is the stator core. This core is typically made from electrical or silicon steel. Additionally, soft magnetic materials such as iron-cobalt or iron-nickel alloys are frequently used to enhance the efficiency of EVs. SMC materials are the latest technology for EVs core application that offers the highest efficiency of the axial flux motor. It can increase motor efficiency to approximately 99% due to its unique characteristics, i.e. the isotropic magnetic behavior, high electrical resistivity, high magnetic permeability, low eddy current loss, low total core loss at low to high frequency, and low magnetic coercivity [9], [10], [11]. SMC is a composite material consisting of ferromagnetic powder particles where each powder particle is isolated by a layer or film consisting of a mixture of other materials [9], [12], [13].

SMC was developed using iron powder as the base material, and efforts have been made to improve the performance of iron-based SMC [14], [15]. Some iron-based SMC were produced commercially, but most are not readily available in Indonesia. In line with these results, Indonesia has great potential in developing iron powder-based SMC because the natural resources of iron minerals are quite large. However, obtaining iron powder with high purity requires a complex production process and high costs. Therefore, there is a need for research on alternative materials to iron powder. When compared with iron powder which is often used as SMC, iron nitride material has a comparable magnetic property [16], [17]. Iron nitride is a transition metal material that has a metastable phase. This is because iron nitride has several phases when it is in the form of bulk, thin film, and powder [18].

The formation of the iron nitride phase is affected by the concentration of nitrogen used. Magnetic properties of iron nitride are excellent for SMC applications, and some iron nitride phases have soft magnetism such as Fe_3N, Fe_4N, and Fe_8N [18], [19], [20]. Iron nitride can be manufactured using various raw materials and methods. Its production is primarily based on conventional nitriding techniques, which are commonly used in alloy steel processing [21]. Therefore, ball milling, gas nitriding, and plasma nitriding are widely applied for the synthesis of iron nitride [19], [22], [23]. Ion nitride with Fe_3N phase can be synthesized using Fe_3O_4 powder as the starting material [24]. From previous research, it was also found that Fe_2O_3 and Fe_3O_4 powder can be derived from natural iron sand using the coprecipitation method [25], [26], [27], [28], [29]. Recently, many efforts have been done for incorporating natural resources in Indonesia, namely iron sands, for magnetic application [27], [30], [31], [32].

Research on natural iron sand-based iron nitride could be highly significant, particularly given Indonesia's abundant iron sand resources. Iron nitride, particularly if derived from locally available iron sand, could offer several advantages in terms of local resource utilization, economic development, environmental sustainability, and technological innovation. The objective of this research is to synthesize iron nitride material using the abundant natural iron sand found in Indonesia. These results constitute a significant stride towards the development of locally sourced SMC material, with prospective applications in EVs.

2. Methods

This research synthesized iron nitride material from iron oxide i.e. Fe_3O_4 and Fe_2O_3. Iron oxide Fe_3O_4 was extracted from natural iron sand obtained in a domestic market in Surabaya, East Java, Indonesia. The synthesis method followed the approach reported in the reference [25]. Magnetic separation is a crucial step in obtaining iron sand with a high Fe_3O_4 content. This enriched material can then be processed further using the coprecipitation method. The coprecipitation method for obtaining magnetite has been used widely [26], [33], [34], to obtain nano-scale powder.

The coprecipitation process started by dissolving iron sand in hydrochloric acid (HCl) under a stirring process at 1000 RPM. Subsequently, ammonium hydroxide (NH_4OH) was added dropwise to the resulting solution to obtain the precipitates. The final stage of the process involved washing and drying the precipitates, resulting in the production of Fe_3O_4 powder. Previous research shows that Fe_2O_3 can be transformed into iron nitride [24], [35]. Therefore, Fe_2O_3 was also used for iron nitride synthesis. Fe_2O_3 powder was produced by heating iron oxide powder Fe_3O_4 phase at a temperature of 600 °C [36], [37].

Gas nitriding was carried out in a tube furnace at different temperatures. Ammonia (NH_3) gas was used during the heating at a flow rate of 150 mL/min. Fe_2O_3 samples were nitrided at temperatures of 600 °C, 625 °C, and 650 °C respectively with a holding time of 4 hours. Gas nitriding

of the Fe_3O_4 sample was carried out at a temperature of 625 °C for 4 hours. The four samples were then expressed by FN1, FN2, FN3, and FN4, respectively.

To analyze the content of the powder obtained, XRD analysis was conducted using Cu-Kα (λ = 1.54060) radiation with a PANalytical Xpert Pro Diffractometer. Natural iron sand was also examined by X-ray Fluorescence (XRF) analysis, using PANalytical MiniPal4. The magnetic properties of the samples were analyzed using Vibrating Sample Magnetometer (VSM) from Dexing Magnet Ltd. VSM250. The surface morphology of nitrided samples was examined using Scanning Electron Microscope (SEM) characterization, equipped with Energy Dispersive Spectroscopy (EDS) using Hitachi FlexSEM 1000.

3. Results and Discussion

3.1. Characterization of Natural Iron Sand

Natural iron sand was used as the raw material for synthesis of iron nitride materials. The synthesis involves coprecipitation and gas nitriding process. The iron sand was purchased from domestic market in Surabaya. The iron sand subsequently underwent some examination prior to coprecipitation process, namely XRD, XRF and SEM. The examinations was carried out to obtain better information regarding the iron sand characteristics.

Figure 1 shows the result of the XRD measurement of the starting material, natural iron sand before magnetic separation. The analysis shows that iron sand contains the Fe_3O_4 phase and there are contaminants in the Ti_2O_3 phase. The Fe_3O_4 and Ti_2O_3 phases was compared with CIF-9009769 and CIF-1532065, respectively. Both phases are common constituents of natural iron sand found in Indonesia, along with Fe_2O_3, SiO_2, Al_2O_3, and TiO_2 [36], [38], [39]. However, Fe_2O_3, SiO_2, Al_2O_3, and TiO_2 were not detected in the XRD measurement. Futher examination in the natural iron sand was carried out using XRF technique to obtain the elemental composition of the iron sand. **Table 1** shows the result of XRF analysis, indicating elemental composition of the iron sand. The XRF result complements the XRD analysis. The main element of the iron sand is iron oxide and titanium oxide, as indicated by the presence of Fe and Ti in the XRF result. Some other elements, such as Al, Si, P, K, Ca, V, Cr, Mn, Cu, Zn, Rb, Zr and Bi, are also detected in a small percentage. The presence of Fe, Ti, Al, Si in the XRF result indicates the typical iron sands obtain from Java, as suggested by works of [40] and [41].

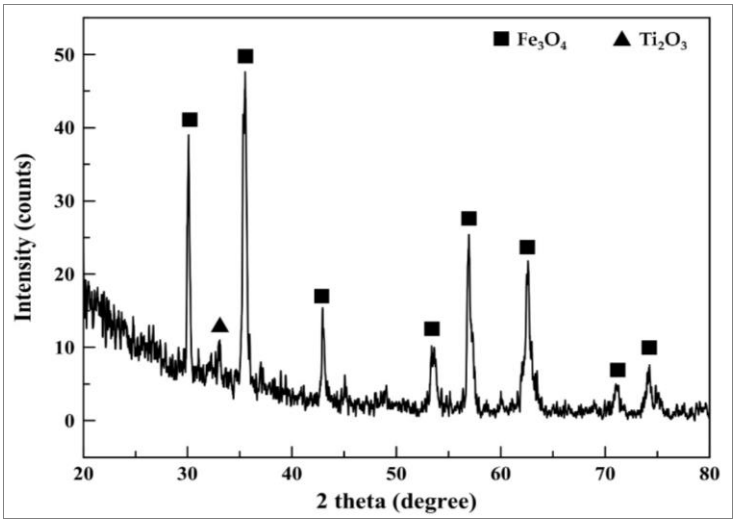

Figure 1. XRD pattern of natural iron sand as starting material

Table 1. Elemental composition of the natural iron sand obtained from XRF analysis, in wt%

Al	Si	P	K	Ca	Ti	V	Cr
0.9	0.9	0.3	0.1	0.27	10	0.51	0.052
Mn	**Fe**	**Cu**	**Zn**	**Rb**	**Zr**	**Bi**	
0.56	86.06	0.071	0.1	0.03	0.03	0.17	

The SEM examination was carried out to investigate the morphology of the iron sand used in the experiment. **Figure 2** shows the microstructure of iron sand, observed using SEM. The morphology of iron sand particles is rounded shape with a smooth surface. The particle size varies between 100 – 400 µm. Natural iron sand in Indonesia has various morphology [39], [42], [43], which includes irregular, rounded, and bitetrahedral shapes, and the surface can be rough or smooth.

3.2. Characterization of Fe_2O_3 and Fe_3O_4 Powders

The characterization shows that the magnetic separation process needs to be improved to eliminate contaminants. The results of the XRD analysis of powder following the process of

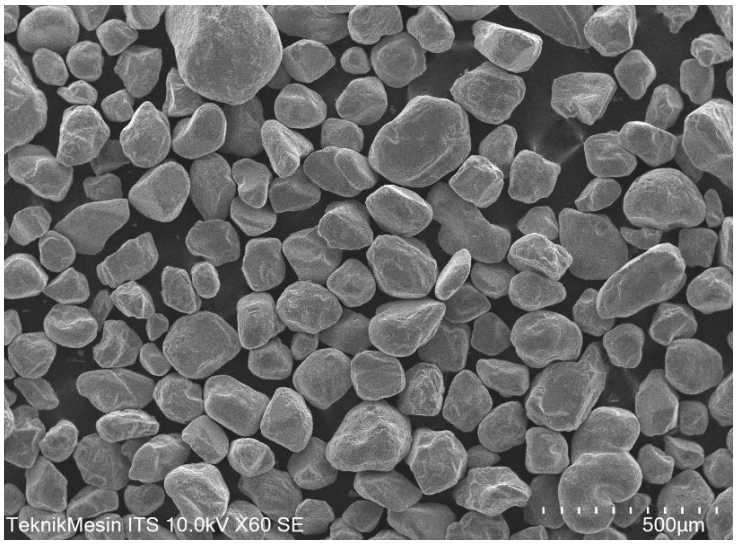

Figure 2. SEM image of the natural iron sands

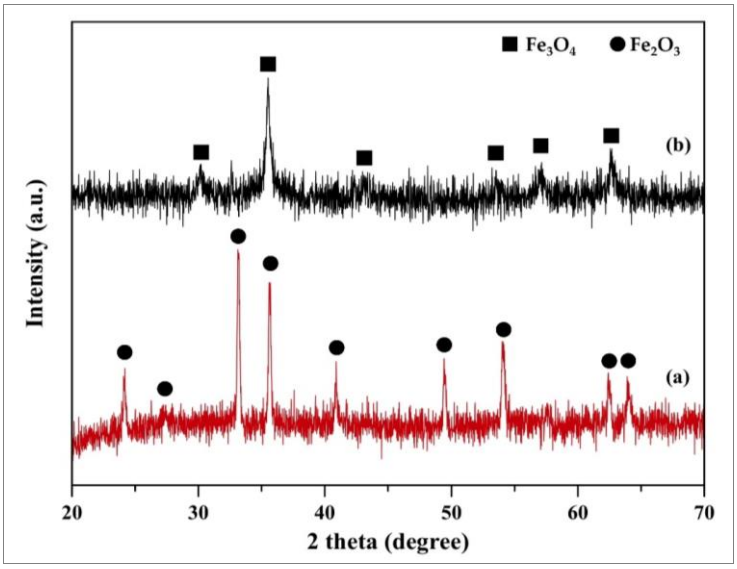

Figure 3. XRD pattern of: (a) Fe_2O_3 powder; (b) Fe_3O_4 powder

coprecipitation and heating of Fe_3O_4 powder are shown in **Figure 3**. The resulting XRD pattern is matched against the CIF data, and quantitative analysis is then performed using MAUD software. After the coprecipitation process, the obtained substance takes the form of Fe_3O_4 powder, possessing the same suitability as CIF-9009769. After the heating process, the Fe_3O_4 powder yields a phase of Fe_2O_3, corresponding to CIF-2101168.

Contaminants in iron sand in the form of Ti_2O_3 phase are not visible in the XRD pattern of Fe_3O_4 powder after the coprecipitation process. The XRD measurement results also show that Fe_2O_3 powder from the oxidation process of Fe_3O_4 powder at a temperature of 600 °C can transform the Fe_3O_4 (magnetite) phase into a single phase Fe_2O_3 (hematite). The result is consistent with the research of [44], [45], [46].

The results of refinement analysis using MAUD software are shown in **Table 2**. It can be seen that the Sigma (Sig) value, reflecting the Goodness of Fitting (GoF), and Rw is in line with the MAUD recommendation. The quantitative analysis derived from MAUD shows information about Fe_2O_3 and Fe_3O_4 powder. The analysis indicates the Fe_3O_4 sample forms a cubic spinel system Fd-3M space group as the phase structure. The Fe_3O_4 has a lattice parameter of 8.3376 Å and a crystal size of 23.7 nm. The experimental result is comparable to the lattice parameter of Fe_3O_4 reported by reference work used [25] in this coprecipitation process. The crystal size of the Fe_3O_4 in this experiment is lower than the reference work. It is likely due to the difference of pH during coprecipitation process. The size of the crystal is influenced by pH of the process. Higher pH tends to produce smaller crystal size, as reported by Sunaryono *et al*. [25] and Kristina *et al*. [47].

Fe_2O_3 nano powders can be sythesized using various methods, as reported by Novita *et al*. [48]. In this experiment, the Fe_2O_3 was produced by heating Fe_3O_4 nano powders, obtained in the coprecipitation process, in a muffle furnace at 600 °C. The XRD result indicates that the Fe_2O_3 has a rhombohedral crystal system with space group of R-3c. The lattice parameter of Fe_2O_3 measures a = 5.03103 Å and c = 13.7014 Å, with a crystal size of 55.9 nm. The lattice parameter result is similar to that reported by other works [29], [49]. The experiment produced Fe_2O_3 powder that has larger crystal size in comparison to the Fe_2O_3 synthesized by coprecipitation method [29], [48], [49]. Larger crystal size obtained in this experiment is obviously caused by the use of heating method in the synthesize of Fe_2O_3 powder. Tulebayeva *et al*. reported that higher annealing temperatures result in larger average nanoparticle sizes [50]. In the study, the starting material of Fe_3O_4 (magnetite), with a crystal size of 12.4 nm, was transformed into Fe_2O_3 (hematite), with a crystal size of 34.6 nm, after the annealing process at 600 °C [50]. The result shows an increase in crystal size during the heating of the Fe_3O_4 powder.

Table 2. Refinement results of the Fe_2O_3 and Fe_3O_4 powder using MAUD analysis

Powder	Data Reference	Space Group	%Wt	Lattice Parameter (Å)		Crystal Size (nm)	RB (%)	Rexp (%)	Rwp (%)	Sig
				a	c					
Fe_2O_3	CIF – 2101168	R -3 c	100	5.03103	13.7014	55.9	9.64	4.84	11.48	2.37
Fe_3O_4	CIF - 9009769	F d -3 m	100	8.3367		23.7	3.80	4.24	4.81	1.13

Based on the XRD analysis, both iron oxide powders can be regarded as nano-sized powders. In general, nano-sized particles have a beneficial effect on the reaction kinetics [51], [52], [53]. Nano-sized particles exhibit significantly higher surface area-to-volume ratios compared to larger particles. Therefore, a faster reaction rate, enhanced diffusion, and improved reactivity are expected [51], [52].

3.3. Synthesis of Iron Nitride

The result of the XRD measurement of the powders after the gas nitriding process is shown in **Figure 4**. The XRD results show that iron nitride can be synthesized using the gas nitriding method. Additionally, successful synthesis of iron nitride has been achieved, forming Fe_3N and Fe_4N. However, there are still contaminants from the sample in the form of Fe_2O_3 and Fe_3O_4. Since the formation of the two phases is also due to a non-optimal process of nitriding ammonia on the powder, contaminants are present in the powder after treatment.

Quantitative analysis was carried out using MAUD software to determine the phase composition formed in the sample. The comparison of phase compositions in the samples is shown in **Table 3**. In the results of the nitriding process, FN2 exhibits relatively fewer contaminants compared to other temperature variations. FN3 on the other hand, shows suboptimal results due to the predominance of contaminants over the formed iron nitride phase. The optimal temperature for forming the Fe_3N phase is found to be 625 °C. Consequently, FN4 yields phases of Fe_4N and Fe_3N. This result is in line with prior research [18], which suggests that the Fe_4N phase can arise from the Fe_3N phase transformation.

Iron nitride is conventionally formed as a result of the interaction of ammonia (NH_3) with the solid iron precursor at temperatures ≥ 400 °C. Both iron precursor and the resulting nitride phases act as catalysts, facilitating the dissociation of NH_3 into atomic nitrogen and subsequently into molecular nitrogen and hydrogen. Nitridation occurs as atomic nitrogen diffuses into the metal, converting it into iron nitride. The extent of nitridation is influenced by reaction temperature and the flow rate of NH_3 gas. Recent work by Jovičević-Klug *et al*. [35] shows the transformation of iron oxide to iron nitride. The formation of iron nitride is likely to occur through a stepwise reduction of iron oxide rather than a direct transformation from oxide to nitride.

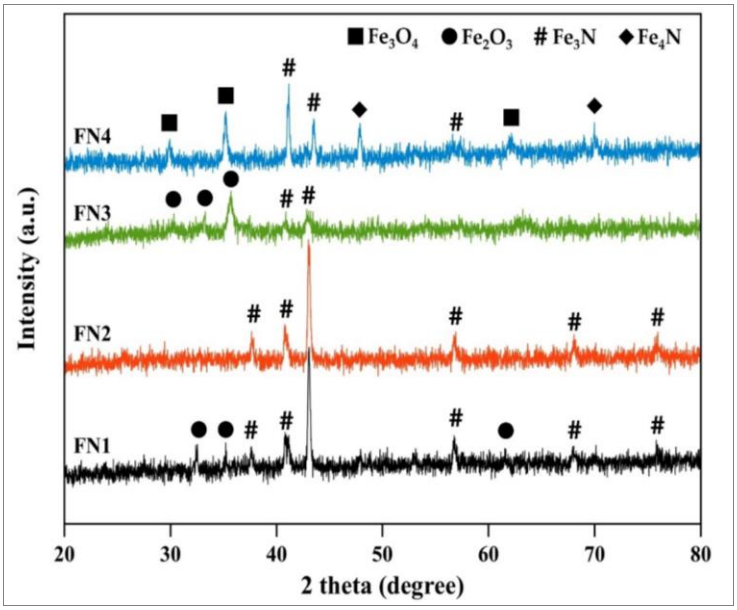

Figure 4. XRD patterns of FN1, FN2, FN3 and FN4 samples

Table 3. Comparison of the number of phases formed in each variation using MAUD analysis

Sample	Variation	Composition			
		Fe_2O_3	Fe_3O_4	Fe_3N	Fe_4N
FN1	Fe_2O_3 nitriding temperature 600 °C	19.79 %	-	80.21%	-
FN2	Fe_2O_3 nitriding temperature 625 °C	7.34%	-	92.66%	-
FN3	Fe_2O_3 nitriding temperature 650 °C	79.24%	-	20.76%	-
FN4	Fe_3O_4 nitriding temperature 625 °C	-	46.51%	21.8%	31.69%

SEM examination equipped with EDS analysis was carried out on samples of FN2 and FN4 as shown in **Figure 5**. From the SEM morphology results, it was shown that the particles in the two

powders had irregular shapes, which are formed due to the formation of the iron nitride phase. **Figure 6** shows that the morphology has an irregular lamellar texture. The irregular shape of iron nitride was reported in the previous investigation [24]. Similar morphology of iron nitride is reported in the works of Zhang *et al*. [19], Gang *et al*. [48] and Liu *et al*. [54]. The reference works reported that the iron nitride has irregular spherical or ellipsoidal shape as its final form. The irregular lamellar texture of iron nitride in the FN4 sample is more profound than the one in the FN2 sample. Another structure that can be seen in the SEM result is iron oxide. The initial fine shape of iron oxide powder becomes coarse and changes the nitriding process [19], [24], [55].

EDS analysis on both samples shows that the structure is iron nitride, as shown in **Figure 6**. Although EDS analysis detected trace amounts of Ti, Al, and Cu, these elements were not observed in the XRD patterns. This discrepancy is attributed to the higher surface sensitivity of EDS, which can detect elemental residues or minor surface contaminants not present in significant crystalline phases. Since XRD only detects well-crystallized phases above a certain concentration threshold (~2–5 wt%), the absence of the trace elements peaks suggests that these elements are either amorphous or below detection limits.

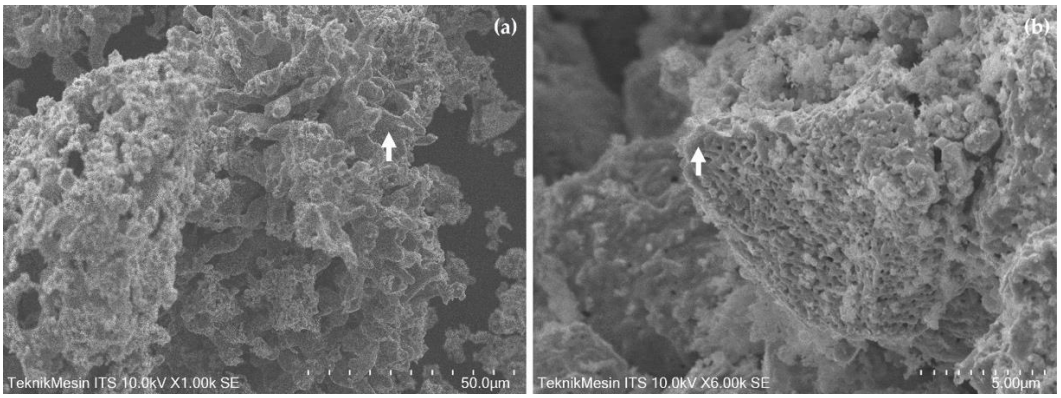

Figure 5. SEM image of iron nitride samples. The arrow shows the location of the EDS spot analysis: (a) FN2 sample; (b) FN4 sample

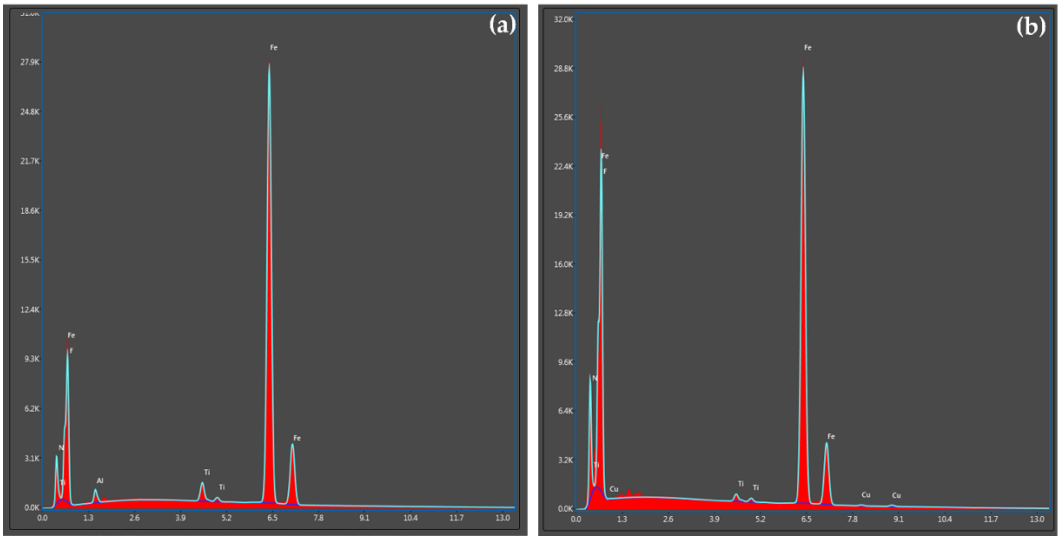

Figure 6. EDS results of the iron nitride samples. Location of EDS spot analysis is indicated in **Figure 5**: (a) FN2 sample; (b) FN4 sample

The magnetic properties of iron nitride powder can be seen from the results of the VSM analysis in the form of a hysteresis loop. The hysteresis loop of the samples is shown in **Figure 7**. Magnetic saturation value of FN4 was 75.41 emu/g. The saturation magnetic values of FN1, FN2, and FN3 were 28.6 emu/g; 33.94 emu/g; and 18.9 emu/g, respectively. The result of FN4 has the highest magnetic saturation value compared to the results of FN1, FN2, and FN3 because the Fe_4N phase is formed in the gas nitriding process. The lowest magnetic saturation value is obtained in the FN3 sample, which consists of more Fe_2O_3 than iron nitride. Therefore, a lower magnetic saturation value is achieved. The value of saturation magnetization, retentivity, and coercivity is listed in **Table 4**.

The value of magnetization is related to the number of phases present in the samples. As shown in **Table 3**, the FN4 sample consists of Fe_3O_4, Fe_3N, and Fe_4N. The FN2 sample contains only Fe_2O_3 and Fe_3N. Fe_4N has larger magnetization than Fe_3N [16], [18]. Therefore, the FN4 has a larger magnetic saturation value than the FN2 sample. The magnetization value of all samples is lower

than the result reported by other studies [17], [19], [20], [56]. The lower value obtained in this study is caused by the presence of contaminants in the form of the initial sample phases, namely Fe_2O_3 and Fe_3O_4. Magnetic saturation values of the two phases are smaller than the results of Fe_3N [23] and Fe_4N [57]. The effect of contaminants on magnetic saturation value has been reported in [39], and [40]. The decrease in magnetic saturation of the samples is attributed to the presence of contaminants i.e. Fe_2O_3 and Fe_3O_4.

The coercive fields of each sample FN1, FN2, FN3, and FN4 are 94.29 Oe, 104.94 Oe, 386.53 Oe, and 137.63 Oe. The highest coercivity value is on FN3, and the lowest is on FN1. In principle, the coercivity value of the iron nitrides samples is higher than typical soft magnetic materials. From the results of the coercivity field, it can be observed that coercivity increases with the rise in nitriding temperature. Based on the XRD analysis, listed in **Table 3**, higher nitriding temperature yields lower amount of Fe_3N. Since Fe_3N is considered to have soft magnetic behaviour, the decrease of its amount will surely effect the coercivity. Similar tendency in coercivity is also reported by Palade *et al*. [58].

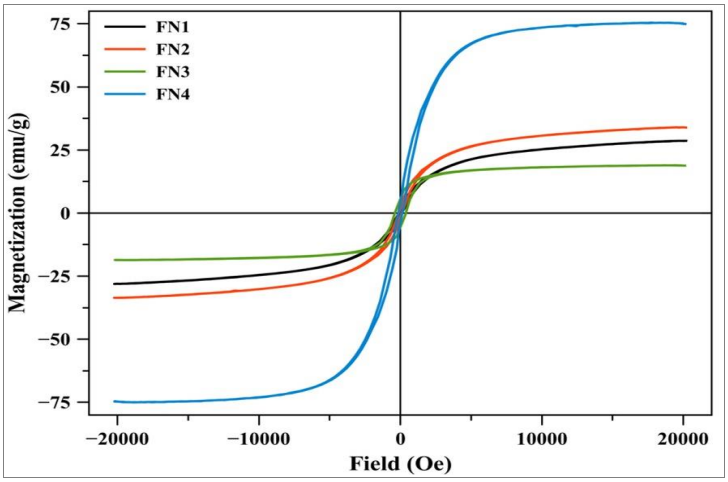

Figure 7. Hysteresis curve of iron nitride powders (FN1, FN2, FN3, and FN4)

Table 4. Magnetic properties of iron nitride powders (FN1, FN2, FN3, and FN4)

Sample	Saturation Magnetization (emu/g)	Retentivity (emu/g)	Coercivity (Oe)
FN1	28.6	0.93	94.29
FN2	33.94	1.43	104.94
FN3	18.9	5.55	386.53
FN4	75.41	3.89	137.63

4. Conclusion

In conclusion, iron nitride was successfully synthesized from natural iron sand using coprecipitation and gas nitriding methods. Nitriding Fe_2O_3 powder yielded the Fe_3N phase, while nitriding Fe_3O_4 powder yielded both the Fe_4N and Fe_3N phases. These results showed the presence of contaminants in the initial powder phase. The presence of these phases was attributed to suboptimal conditions during the gas nitriding process. Surface morphology analysis equipped with EDS analysis showed that iron nitride has irregular shapes, typically irregular lamellar structures. VSM testing showed that the FN4 sample has the highest magnetic saturation i.e., 75.41 emu/g. The lowest magnetic saturation was obtained in the FN3 sample with a value of 18.9 emu/g. All samples yielded lower magnetization than results reported by other investigations. The lower magnetization value was attributed to the presence of contaminants such as Fe_2O_3 and Fe_3O_4. Gas nitriding parameters must be optimized in order to obtain only iron nitride phases, specifically Fe_4N.

Authors' Declaration

Authors' contributions and responsibilities - The authors made substantial contributions to the conception and design of the study. The authors took responsibility for data analysis, interpretation and discussion of results. The authors read and approved the final manuscript.

Funding – No funding information from the authors.

Availability of data and materials - All data is available from the authors.

Competing interests - The authors declare no competing interests.

Additional information – No additional information from the authors.

References

[1] M. N. Yuniarto, I. Sidharta, S. E. Wiratno, Y. U. Nugraha, and D. A. Asfani, "Indonesian Electric Motorcycle Development: Lessons from innovation-based concept implementation on the design and production of the first Indonesian electric motorcycle," *IEEE Electrification Magazine*, vol. 10, no. 1, pp. 65–74, Mar. 2022, doi: 10.1109/MELE.2021.3139247.

[2] M. N. Yuniarto, Y. U. Nugraha, I. M. Y. Negara, D. A. Asfani, and I. Sidharta, "Designing and performance investigation of permanent magnet motor prototype for UTV electric drive train application," *International Journal of Power Electronics and Drive Systems (IJPEDS)*, vol. 12, no. 4, p. 2018, Dec. 2021, doi: 10.11591/ijpeds.v12.i4.pp2018-2029.

[3] D. A. Asfani *et al.*, "Electric Vehicle Research in Indonesia: A Road map, Road tests, and Research Challenges," *IEEE Electrification Magazine*, vol. 8, no. 2, pp. 44–51, Jun. 2020, doi: 10.1109/MELE.2020.2985485.

[4] M. Butcher, "Acquired by Mercedes-Benz, YASA's revolutionary electric motor is set for big things," TechCrunch. Accessed: Feb. 10, 2025. [Online]. Available: https://techcrunch.com/2021/09/03/acquired-by-mercedes-benz-yasas-revolutionary-electric-motor-is-set-for-big-things/

[5] B. Oliver, "An Innovative EV Motor Used by Lamborghini, McLaren, and Ferrari Is Being Mass-Produced by Mercedes," Wired. Accessed: Feb. 10, 2025. [Online]. Available: https://www.wired.com/story/yasa-motors-mercedes-axial-flux-2024/

[6] A. F. Desanti, D. A. Asfani, M. N. Yuniarto, and Y. U. Nugraha, "Comparison and Analysis of Stator Plate Holder on Yokeless and Segmented Armature Machine," *Journal of Physics: Conference Series*, vol. 1577, no. 1, p. 012039, Jul. 2020, doi: 10.1088/1742-6596/1577/1/012039.

[7] Y. U. Nugraha, D. Anton Asfani, D. C. Riawan, and M. Nur Yuniarto, "Performance Improvement of Axial Switched Reluctance Motor using Low-Cost Magnet," in *2019 6th International Conference on Electric Vehicular Technology (ICEVT)*, IEEE, Nov. 2019, pp. 300–303. doi: 10.1109/ICEVT48285.2019.8994021.

[8] A. Multi, I. Garniwa, and U. B. Sudibyo, "Determining the Air Gap Length of an Axial Flux Wound Rotor Synchronous Generator," *MAKARA Journal of Technology Series*, vol. 17, no. 2, Sep. 2013, doi: 10.7454/mst.v17i2.1952.

[9] H. Shokrollahi and K. Janghorban, "Soft magnetic composite materials (SMCs)," *Journal of Materials Processing Technology*, vol. 189, no. 1–3, pp. 1–12, Jul. 2007, doi: 10.1016/j.jmatprotec.2007.02.034.

[10] J. Vesa and P. Rasilo, "Producing 3-D Imitations of Soft Magnetic Composite Material Geometries," *IEEE Transactions on Magnetics*, vol. 55, no. 10, pp. 1–10, Oct. 2019, doi: 10.1109/TMAG.2019.2925580.

[11] K. J. Sunday and M. L. Taheri, "Soft magnetic composites: recent advancements in the technology," *Metal Powder Report*, vol. 72, no. 6, pp. 425–429, Nov. 2017, doi: 10.1016/j.mprp.2016.08.003.

[12] L. Qian, J. Peng, Z. Xiang, Y. Pan, and W. Lu, "Effect of annealing on magnetic properties of Fe/Fe3O4 soft magnetic composites prepared by in-situ oxidation and hydrogen reduction methods," *Journal of Alloys and Compounds*, vol. 778, pp. 712–720, Mar. 2019, doi: 10.1016/j.jallcom.2018.11.184.

[13] Z. Birčáková *et al.*, "Magnetic properties of Fe-based soft magnetic composite with insulation coating by resin bonded Ni-Zn ferrite nanofibres," *Journal of Magnetism and Magnetic Materials*, vol. 485, pp. 1–7, Sep. 2019, doi: 10.1016/j.jmmm.2019.04.060.

[14] A. R. Asari, Y. Guo, and J. Zhu, "Performances of SOMALOY 700 (5P) and SOMALOY 500 Materials under 1-D Alternating Magnetic Flux Density," in *2019 International UNIMAS STEM 12th Engineering Conference (EnCon)*, IEEE, Aug. 2019, pp. 52–58. doi: 10.1109/EnCon.2019.8861264.

[15] Á. S. Muñoz *et al.*, "Study of an iron phosphate soft magnetic composite and its stability at high temperatures," *Ceramics International*, vol. 50, no. 13, pp. 22468–22478, Jul. 2024, doi: 10.1016/j.ceramint.2024.03.349.

[16] X. Tan, S. Wang, Y. Chen, Y. Zhou, and Z. Li, "Design, preparation and characterization of iron

nitride magnetic abrasives," *Journal of Alloys and Compounds*, vol. 774, pp. 443–450, Feb. 2019, doi: 10.1016/j.jallcom.2018.09.389.

[17] C. Zhang *et al.*, "Design, Preparation, and Magnetic Properties of Fe4N/Fe3N Soft Magnetic Composites Fabricated by Gas Nitridation," *Journal of Superconductivity and Novel Magnetism*, vol. 36, no. 3, pp. 923–929, Mar. 2023, doi: 10.1007/s10948-023-06521-8.

[18] S. Bhattacharyya, "Iron Nitride Family at Reduced Dimensions: A Review of Their Synthesis Protocols and Structural and Magnetic Properties," *The Journal of Physical Chemistry C*, vol. 119, no. 4, pp. 1601–1622, Jan. 2015, doi: 10.1021/jp510606z.

[19] C. Zhang *et al.*, "Preparation and soft magnetic properties of γ'-Fe4N particles," *Journal of Materials Science: Materials in Electronics*, vol. 29, no. 2, pp. 1254–1257, Jan. 2018, doi: 10.1007/s10854-017-8029-5.

[20] A.-M. Zieschang *et al.*, "Nanoscale Iron Nitride, ε-Fe 3 N: Preparation from Liquid Ammonia and Magnetic Properties," *Chemistry of Materials*, vol. 29, no. 2, pp. 621–628, Jan. 2017, doi: 10.1021/acs.chemmater.6b04088.

[21] J. Triyono, R. Rahajeng, and E. Surojo, "Surface Modification and Hardness Behavior of AISI 304 as an Artificial Hip Joint using Ammonia and Scallop Shell Powder as a Nitriding Agent," *Evergreen*, vol. 8, no. 2, pp. 335–343, Jun. 2021, doi: 10.5109/4480714.

[22] M. Gong, P. Li, and W. Tong, "Absorption properties of iron nitrides particles fabricated by ball milling," in *2018 International Symposium on Mechanics, Structures and Materials Science (MSMS 2018)*, 2018, p. 020011. doi: 10.1063/1.5048742.

[23] Y. Utsushikawa and K. Niizuma, "The saturation magnetization of Fe□N films prepared by nitriding treatment in N2 plasma," *Journal of Alloys and Compounds*, vol. 222, no. 1–2, pp. 188–192, May 1995, doi: 10.1016/0925-8388(94)04915-7.

[24] I. Sidharta, N. H. Romadhon, R. F. Syah, R. K. Hafiyanda, D. Darminto, and A. Shahab, "Preparation of Iron Nitride Material from Natural Iron Sand," *Materials Science Forum*, vol. 1028, pp. 50–55, Apr. 2021, doi: 10.4028/www.scientific.net/MSF.1028.50.

[25] Sunaryono *et al.*, "Various Magnetic Properties of Magnetite Nanoparticles Synthesized from Iron-Sands by Coprecipitation Method at Room Temperature," *Materials Science Forum*, vol. 827, pp. 229–234, Aug. 2015, doi: 10.4028/www.scientific.net/MSF.827.229.

[26] A. Taufiq, Sunaryono, E. G. Rachman Putra, S. Pratapa, and Darminto, "Nano-Structural Studies on Fe_3O_4 Particles Dispersing in a Magnetic Fluid Using X-Ray Diffractometry and Small-Angle Neutron Scattering," *Materials Science Forum*, vol. 827, pp. 213–218, Aug. 2015, doi: 10.4028/www.scientific.net/MSF.827.213.

[27] Z. Jalil, A. Rahwanto, F. Mulana, and E. Handoko, "Synthesis of nano-hematite (Fe2O3) extracted from natural iron ore prepared by mechanical alloying method," in *Nanoscience and Nanotechnology: NANO-SciTech*, 2019, p. 020041. doi: 10.1063/1.5124671.

[28] M. . Muhammad, A. . Fatmaliana, and Z. . Jalil, "Study of hematite mineral (Fe 2 O 3) extracted from natural iron ore prepared by co-precipitation method," *IOP Conference Series: Earth and Environmental Science*, vol. 348, no. 1, p. 012135, Nov. 2019, doi: 10.1088/1755-1315/348/1/012135.

[29] R. Ramlan, A. A. Bama, A. Johan, M. Naibaho, and M. Ginting, "Synthesis and Characterization of Hematite (α-Fe_2O_3) from Iron Sand Using Coprecipitation Method," *Key Engineering Materials*, vol. 985, pp. 145–151, Aug. 2024, doi: 10.4028/p-uIb7JJ.

[30] N. Novita, M. Naibaho, E. Puspita, R. Ramlan, M. Ginting, and S. Humaidi, "Analysis of Mineral Content and Magnetic Properties of Iron Sand of Bah Bolon Simalungun River, North Sumetera," *Asian Journal of Engineering, Social and Health*, vol. 2, no. 12, pp. 1633–1639, Dec. 2023, doi: 10.46799/ajesh.v2i12.196.

[31] N. R. Ardiani, S. Setianto, B. Santosa, B. M. Wibawa, C. Panatarani, and I. M. Joni, "Quantitative analysis of iron sand mineral content from the south coast of Cidaun, West Java using rietveld refinement method," in *2nd International Conference and Exhibition on Powder Technology (ICePTi)*, 2020, p. 040003. doi: 10.1063/5.0003018.

[32] R. Adi, I. Ismail, A. Akhyar, Z. Jalil, and H. G. Ariel, "Nanomagnetite Extraction from Iron Sand Prepared by Mechanical Alloying Method," *Key Engineering Materials*, vol. 892, pp. 129–133, Jul. 2021, doi: 10.4028/www.scientific.net/KEM.892.129.

[33] S. T. Wicaksono, A. Wahfiudin, A. D. Pramata, and S. Sagadevan, "Effect of Fe (III)/Fe (II) cation

molar ratio variation on magnetite Fe3O4 nanoparticles synthesized from natural iron sand by co-precipitation method," *MRS Advances*, vol. 9, no. 20, pp. 1593–1597, Dec. 2024, doi: 10.1557/s43580-024-00923-z.

[34] Maulinda, I. Zein, and Z. Jalil, "Identification of Magnetite Material (Fe 3 O 4) Based on Natural Materials as Catalyst for Industrial Raw Material Application," *Journal of Physics: Conference Series*, vol. 1232, no. 1, p. 012054, Sep. 2019, doi: 10.1088/1742-6596/1232/1/012054.

[35] M. Jovičević-Klug, Y. Ma, P. Jovičević-Klug, J. M. Prabhakar, M. Rohwerder, and D. Raabe, "Thermal Kinetics and Nitriding Effect of Ammonia-Based Direct Reduction of Iron Oxides," *ACS Sustainable Chemistry & Engineering*, vol. 12, no. 26, pp. 9882–9896, Jul. 2024, doi: 10.1021/acssuschemeng.4c02363.

[36] R. D. Widodo *et al.*, "Synthesis and characterization of iron (III) oxide from natural iron sand of the south coastal area, Purworejo Central Java," *Journal of Physics: Conference Series*, vol. 1444, no. 1, p. 012043, Jan. 2020, doi: 10.1088/1742-6596/1444/1/012043.

[37] A. Jafari, S. Farjami Shayesteh, M. Salouti, and K. Boustani, "Effect of annealing temperature on magnetic phase transition in Fe3O4 nanoparticles," *Journal of Magnetism and Magnetic Materials*, vol. 379, pp. 305–312, Apr. 2015, doi: 10.1016/j.jmmm.2014.12.050.

[38] S. Nengsih, S. N. Madjid, M. Mursal, R. Idroes, and Z. Jalil, "Magnetization Study of Iron Sand from Sabang, Indonesia: The Potential of Magnetic Materials in the Photocatalytic Field," *Bulletin of Chemical Reaction Engineering & Catalysis*, vol. 18, no. 2, pp. 344–352, Aug. 2023, doi: 10.9767/bcrec.19041.

[39] O. Togibasa, S. Bijaksana, and G. Novala, "Magnetic Properties of Iron Sand from the Tor River Estuary, Sarmi, Papua," *Geosciences*, vol. 8, no. 4, p. 113, Mar. 2018, doi: 10.3390/geosciences8040113.

[40] L. Maghfiroh, A. Susilo, Wiyono, and A. N. Faris, "Magnetic mineral characterization of iron sand deposits in Bambang Beach Lumajang, East Java, Indonesia," in *The 3rd International Conference on Science, Mathematics, Environment, and Education*, 2023, p. 100003. doi: 10.1063/5.0106817.

[41] R. . Nathasa, S. . Bijaksana, S. J. . Fajar, and T. G. . Pitaloka, "MAGNETIC AND GEOCHEMICAL CHARACTERIZATIONS OF IRONSAND DEPOSITS FROM CIREBON COASTAL AREA, WEST JAVA," *IOP Conference Series: Earth and Environmental Science*, vol. 873, no. 1, p. 012076, Oct. 2021, doi: 10.1088/1755-1315/873/1/012076.

[42] G. H. . Tamuntuan, A. . Tanauma, G. . Pasau, and H. . Sangian, "Grain size distribution, morphology, and elemental composition of iron sand from North Sulawesi," *IOP Conference Series: Materials Science and Engineering*, vol. 567, no. 1, p. 012042, Jul. 2019, doi: 10.1088/1757-899X/567/1/012042.

[43] E. . Handoko *et al.*, "Structural, magnetic and microwave absorption properties of natural iron sand," *Journal of Physics: Conference Series*, vol. 1869, no. 1, p. 012182, Apr. 2021, doi: 10.1088/1742-6596/1869/1/012182.

[44] Ravita, Amita, A. Kumar, and P. S. . Rana, "Effect of Annealing on Structural Properties of Fe 3 O 4 Ferrite Nanoparticles," *Advanced Science Letters*, vol. 24, no. 8, pp. 5748–5751, Aug. 2018, doi: 10.1166/asl.2018.12190.

[45] N. V. Long, T. N. H. Nguyen, H. P. Le, V. C. Ho, and H. T. Nguyen, "The transformation of ferromagnetic properties of Fe3O4 into ferromagnetic properties of α-Fe2O3 by the polyol process, heat treatment, isothermally annealing and sintering," *Communications in Physics*, vol. 34, no. 3, p. 3\, Jul. 2024, doi: 10.15625/0868-3166/20630.

[46] M. K. . Srivastava and U. Kumar, "Structural and optical properties of α -Fe 2 O 3 nanoparticles realized by simple thermal decomposition route," *Physica Scripta*, vol. 96, no. 1, p. 015804, Nov. 2020, doi: 10.1088/1402-4896/abc281.

[47] N. P. D. Kristina, I. G. Arjana, and P. Yasa, "SYNTHESIS AND CHARACTERIZATION OF MAGNETITE NANOMATERIALS IN TIANYAR IRON SAND USING CO-PRECIPITATION METHOD," *Indonesian Physical Review*, vol. 7, no. 3, pp. 398–413, Jul. 2024, doi: 10.29303/ipr.v7i3.328.

[48] N. Novita, R. Ramlan, M. Naibaho, M. Ginting, S. Humaidi, and T. N. Duma, "Fe2O3 Review: Nanostructure, Synthesis Methods, and Applications," *International Journal of Social Service and Research*, vol. 4, no. 02, pp. 539–559, Feb. 2024, doi: 10.46799/ijssr.v4i02.728.

[49] P. M. Parvathy Namboothiri and M. . Vasundhara, "Synthesis and characterization of nano-

hematite," *Materials Today: Proceedings*, vol. 92, pp. 1459–1463, 2023, doi: 10.1016/j.matpr.2023.05.652.

[50] D. Tulebayeva, A. Yermekova, A. Kozlovskiy, and M. Zdorovets, "Investigation of phase transformations of iron nanoparticles during thermal annealing," *EPJ Web of Conferences*, vol. 201, p. 02003, Feb. 2019, doi: 10.1051/epjconf/201920102003.

[51] Q.-S. Fu, Y.-Q. Xue, Z.-X. Cui, and M.-F. Wang, "Study on the Size-Dependent Oxidation Reaction Kinetics of Nanosized Zinc Sulfide," *Journal of Nanomaterials*, vol. 2014, no. 1, p. 856489\, Jan. 2014, doi: 10.1155/2014/856489.

[52] S. H. Kayani, H. M. S. Ajmal, B.-J. Kim, N.-K. Park, and K. Euh, "Influence of Powder Size on Pore Characteristics and Intermetallic Phase Kinetics in Porous Ti-Al Alloys," *Crystals*, vol. 14, no. 6, p. 559, Jun. 2024, doi: 10.3390/cryst14060559.

[53] A. Albrecht and D. Moszyński, "Nitriding and Denitriding of Nanocrystalline Iron System with Bimodal Crystallite Size Distribution," *Materials*, vol. 15, no. 1, p. 143, Dec. 2021, doi: 10.3390/ma15010143.

[54] Y. Liu, Z. Yang, and H. Yang, "Magnetic and Electrochemical Properties of γ′-Fe 4 N Nanoparticles with Cuboidal and Rodlike Morphologies," *The Journal of Physical Chemistry C*, vol. 127, no. 1, pp. 728–735, Jan. 2023, doi: 10.1021/acs.jpcc.2c07335.

[55] M. Yu, Y. Xu, Q. Mao, F. Li, and C. Wang, "Electromagnetic and absorption properties of nano-sized and micro-sized Fe 4 N particles," *Journal of Alloys and Compounds*, vol. 656, pp. 362–367, Jan. 2016, doi: 10.1016/j.jallcom.2015.10.005.

[56] W. Yin *et al.*, "Soft magnetic ε-Fe3N: Synthesis, characterization and magnetic properties," *Journal of Alloys and Compounds*, vol. 688, pp. 828–832, Dec. 2016, doi: 10.1016/j.jallcom.2016.07.104.

[57] T. . Yamaguchi, M. . Sakita, M. . Nakamura, and T. . Kobira, "Synthesis and characteristics of Fe4N powders and thin films," *Journal of Magnetism and Magnetic Materials*, vol. 215–216, pp. 529–531, Jun. 2000, doi: 10.1016/S0304-8853(00)00210-9.

[58] P. Palade *et al.*, "Structural, Magnetic, and Mössbauer Investigation of Ordered Iron Nitride with Martensitic Structure Obtained from Amorphous Hematite Synthesized via the Microwave Route," *Industrial & Engineering Chemistry Research*, vol. 56, no. 11, pp. 2958–2966, Mar. 2017, doi: 10.1021/acs.iecr.6b04574.